



Explicit Formulations of Mass and Stiffness Matrices for Vibration Analysis of Tapered Elements

Khaled M. Ahmida

Faculty of Engineering, University of Tripoli
k.ashouri@uot.edu.ly

Abstract—This paper presents explicit formulations to calculate the mass and stiffness matrices used in the finite element method for vibration analysis in rod, beam, and shaft tapered elements. The cross-sections of these elements are considered to vary linearly. The analyses of two types of cross-sections are carried out; the circular cross-section and the rectangular cross-section. The shape functions are formulated for each type of elements. The presented formulations are straightforward to use in a piecewise form. As an acceptable alternative, the obtained expressions are benchmarked by replacing the tapered member with a sufficient number of rigidly connected uniform elements. The comparison is made between the obtained modal parameters, mainly the natural frequencies of the analyzed element. The obtained results are accurate and confirm the reliability of the presented formulations.

Index Terms: Tapered finite element, FEA, 3D truss elements, vibration analysis.

I. INTRODUCTION

Tapered elements are needed in many structures, where the distribution of loads and weights is required to respect a certain pattern. The tapered elements have a desirable structural efficiency, which is mainly the high stiffness-to-mass ratio. They have the advantage of providing better shear-carrying capacity and high lateral stability when compared to uniform elements, besides weight saving. There are a variety of tapered elements regarding their cross-section variations. Tapered elements can have circular, rectangular, or even I-shaped, H-shaped cross-sections. The cross-section variations for all these types, depending on their type, could be simplified by considering a linear or polynomial variation of the cross-section along the element axis. A simple technique, if, say, a beam element is used, to analyze the tapered element is to divide it into several uniform straight beam elements [1]. This methodology is not as accurate as using a specific tapered element instead. Some previous work was done utilizing the Bessel function type of

solution for the tapered element [2]. The governing equation for tapered elements can be solved analytically [3,4], but a matrix representation is needed when dealing with complex structures. Langley [5] conducted an extensive investigation on wave propagation in non-homogeneous waveguides, where longitudinal and flexural motions are considered. An approximate method, proposed by Bazeos [6], is based on using a series of dimensionless design-oriented charts relating the critical load of linearly tapered columns.

Nevertheless, few approaches separately address the use of direct expressions for the analysis of the members that constitute a 3D truss structure, which involves axial, flexural, and torsional vibrations. Cem Ece et al. [7] have investigated the vibration of a beam with a variable cross section, where the change in area was formulated using a non-uniformity parameter given as an exponential function. Different boundary conditions were analyzed. No expressions were given for the mass and stiffness matrices, but instead the natural frequencies and mode shapes were calculated. The linearly tapered Timoshenko beam was studied by Huong and Gan [8], where its shape functions were developed. The shape functions were verified by performing a static analysis of a tapered element. Mohri et al. [9] investigated the case of large torsion of a thin-walled tapered beam element, and studied the buckling in these types of structures. Kalkowski et al. [10] analyzed longitudinal wave propagation in a varying cross section rod, exponentially tapered. It concentrated on cut-off frequency at which the longitudinal waves start to propagate in the rod. The work was supported experimentally. Later in 2019, Banerjee and Ananthapuvirajah [11] investigated an analytical procedure to compute the natural frequencies and mode shapes of tapered beams, with solutions based on the Bessel function. However, no closed-form expressions were presented for the mass and stiffness matrices. Chockalingam et al. [12] studied tapered I-beams focusing on shear stress distribution, presented analytical solutions and validated with the finite element method. Lateral buckling analysis was conducted on sandwich fiber-metal laminate tapered I-beams [13].

Received 27 Feb, 2023; revised 21 Mar, 2023; accepted 25 Apr, 2023.

Available online 28 Feb, 2023.

The structure was subjected to transverse loading, with results verification using ANSYS package.

In this paper, an attempt is provided to obtain closed expressions for mass and stiffness matrices, put in simpler manner, for tapered elements analysis. Two special types of tapered cross-sections, circular and rectangular types, are formulated. These solutions are provided for beam, rod, and shaft finite elements, considering a linear variation of their cross-sections. These types of waveguides are selected because together they facilitate the study of vibrations of 3D truss-type structures that might have tapered elements.

II. LINEARLY TAPERED ELEMENTS: CIRCULAR CROSS-SECTIONS

The equations describing how the element cross-section varies along its axis are described as follows. Beginning with the linear change of radius, the following equation can be adopted,

$$r(x) = r_0 \left(1 + \frac{c_1 x}{L} \right), \quad (1)$$

where $r(x)$ is the radius for radius linear variation with beam axis, r_0 is the radius at $x=0$, r_L is the radius at $x=L$, L is the length of the element, and c_1 is a constant found by applying the boundary conditions defined as $r(\text{at } x = 0) = r_0$, and $r(\text{at } x = L) = r_L$. Thus, the radius variation function becomes,

$$r(x) = \frac{(L-x)r_0 + x r_L}{L}. \quad (2)$$

Therefore, the functions that describe the change of the circular cross-section area $A(x)=\pi r(x)^2$, the moment of inertia $I(x)=\pi r(x)^4/4$, and the polar moment of inertia $J(x)=\pi r(x)^4/2$ can be finally written as follows, respectively,

$$A(x) = \frac{\pi((L-x)r_0 + x r_L)^2}{L^2}, \quad (3)$$

$$I(x) = \frac{\pi((L-x)r_0 + x r_L)^4}{4L^4}, \quad (4)$$

$$J(x) = \frac{\pi((L-x)r_0 + x r_L)^4}{2L^4}. \quad (5)$$

These expressions are then used to obtain the shape functions, and consequently the stiffness and mass matrices for the element in question. In the following sections, note that the nodal cross sectional areas are A_0 at $x=0$ and A_L at $x=L$, the nodal moments of inertia are I_0 at $x=0$ and I_L at $x=L$, and the nodal polar moments of inertia are J_0 at $x=0$ and J_L at $x=L$.

A. Beam Tapered Element with Circular Cross-section

Stiffness and mass matrices for a single tapered beam element are formulated. The beam theory considered here is Bernoulli Euler's, see Figure. 1. Note that v_1 and ϕ_1 are the nodal displacement and rotation at node 1, respectively, and v_2 and ϕ_2 are the nodal displacement and rotation at node 2 of the beam element.

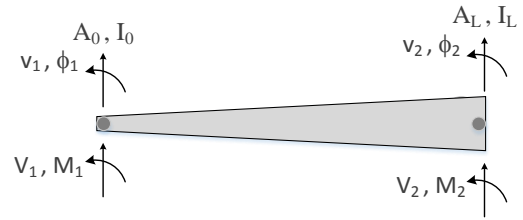


Figure 1. Tapered beam with linear cross-section profile.

In general, for a straight beam, the stiffness and mass matrices can be derived by integrating the governing differential equations of the beam [14, 15]. From the first governing equation, we have

$$E(x)I(x) \frac{d^4 v(x)}{dx^4} = 0, \quad (6)$$

which has a general solution for the transverse displacement in the form

$$v(x) = \alpha_0 + \alpha_1 x + \alpha_2 x^2 + \alpha_3 x^3. \quad (7)$$

Using the end conditions at $x=0$ and at $x=L$, with L as the beam length, and defining the four nodal degrees of freedom for nodal displacements and rotations, respectively, v_1, v_2, ϕ_1, ϕ_2 , we end up with the relation,

$$v(x) = N_1 v_1 + N_2 \phi_1 + N_3 v_2 + N_4 \phi_2, \quad (8)$$

where $N_i(x)$ are defined as the interpolation functions. In the same fashion, the slope, moment $M(x)$ and shear force $V(x)$ are obtained using the governing equation, with E being Young's modulus,

$$M(x) = E(x)I(x) \frac{d^2 v(x)}{dx^2} = E(x)I(x) [N_1''(x)v_1 + N_2''(x)\phi_1 + N_3''(x)v_2 + N_4''(x)\phi_2]. \quad (9)$$

For the beam in Fig. 1, with shear forces $V_1=-V(0)$ and $V_2=+V(L)$, bending moments $M_1=-M(0)$ and $M_2=+M(L)$, the nodal forces and moments can therefore be related to the nodal translations and rotations and put in matrix form.

Following this procedure for a linearly tapered beam element, where the variables $A(x)$ & $I(x)$ are functions of x , and E & ρ are not, the obtained interpolation functions are,

$$N(x) = \begin{Bmatrix} \frac{2x^3}{L^3} - 3\frac{x^2}{L^2} + 1 \\ \frac{x^3}{L^2} - 2\frac{x^2}{L} + x \\ -\frac{2x^3}{L^3} + 3\frac{x^2}{L^2} \\ \frac{x^3}{L^2} - \frac{x^2}{L} \end{Bmatrix}^T. \quad (10)$$

Therefore, and by definition [14], the [4x4] stiffness and mass matrices can be obtained by, respectively,

$$K_B^{Lc} = \int_0^L E(x) I(x) N''^T(x) N''(x) dx, \quad (11)$$

$$M_B^{Lc} = \int_0^L \rho(x) A(x) N^T(x) N(x) dx. \quad (12)$$

Solving these integrals, the elements of the two matrices for the linearly tapered beam element are obtained and given in Appendix A. Both matrices are symmetric.

B. Rod Tapered Element with Circular Cross-section

Stiffness and mass matrices for a single tapered rod element are formulated. The same variables are defined for the areas at the tips $A(x)$. In general, for a straight bar, the stiffness and mass matrices are derived by integrating the governing differential equations for axial deformation. Using a linear equation for the solution of displacements, we end up with linear shape functions: $N_1 = -x/L + 1$, $N_2 = x/L$. Defining the axial forces at the two nodes, and their corresponding displacements, the stiffness and mass matrices can easily be found, in a similar fashion used for beam elements, as following,

$$K_R^{Lc} = \int_0^L E(x) A(x) N'^T(x) N'(x) dx, \quad (13)$$

$$M_R^{Lc} = \int_0^L \rho(x) A(x) N^T(x) N(x) dx. \quad (14)$$

Solving these integrals, the elements of the two matrices for the linearly tapered beam element are obtained and given in Appendix A. Both matrices are symmetric.

C. Shaft Tapered Element with Circular Cross-section

For the shaft tapered element with a circular cross-section, the formulation is obtained following the same procedure as is done for the rod element. The difference here is that the DOFs are torsional displacements and torque forces, obeying the shape function of the rod element. The stiffness and mass matrices are obtained by replacing $E(x)A(x)$ and $\rho(x)A(x)$ for rod element, with $G(x)J(x)$ and $\rho(x)J(x)$ respectively. These matrices, i.e., K_S^{Lc} and M_S^{Lc} are given in Appendix A.

III. LINEARLY TAPRED ELEMENTS: RECTANGULAR CROSS-SECTIONS

In this case, the element cross-section has a rectangular shape, having a fixed height and a varying width, or vice versa. The equation describing the variation of the cross-section area is thus linear, given by,

$$A(x) = \frac{(L-x)A_0 + xA_L}{L}. \quad (15)$$

For the moment of inertia, and as the width of the element changes linearly, a linear function described before for the linear change of radius in circular elements is again adopted. The polar moment of inertia would have a similar equation.

$$I(x) = \frac{(L-x)I_0 + xI_L}{L}, \quad (16)$$

$$J(x) = \frac{(L-x)J_0 + xJ_L}{L}. \quad (17)$$

A. Beam, Rod, and Shaft Tapered Elements with Rectangular Cross-section

Beam element: the shape functions are still the same for the beam element given above. The stiffness and mass matrices for this type of cross-section are symmetric. They are obtained using equations (11) and (12), together with equations (15) and (16). The terms of matrices K_B^{Lr} and M_B^{Lr} are shown in Appendix B.

Rod element: adopting the same shape functions for the rod element above, and using equation (15) in equations (13) and (14), we end up with the stiffness and mass matrices K_R^{Lr} and M_R^{Lr} , respectively, as shown in Appendix B.

Shaft element: using similar expressions used for the rod element, but replacing $E(x)A(x)$ and $\rho(x)A(x)$ with $G(x)J(x)$ and $\rho(x)J(x)$ respectively, and solving the integrals, we obtain the matrices K_S^{Lr} and M_S^{Lr} as given in Appendix B.

IV. NUMERICAL EXPERIMENT OF THE OBTAINED FORMULAS

All obtained matrices are verified in what follows. Straight tapered models of a beam, rod, and shaft elements are used. All three models have stainless steel elements of $E=200\text{GPa}$, $\rho = 7850\text{kg/m}^3$, $\nu = 0.3$, and a total length of 1m. All models represent a cantilever member, fixed at the smaller cross-section area $A(x=0)$, see Figure 2. An impulse load of unitary value is applied at the free tip, being a transversal excitation in the case of a beam, axial for a rod, and torque for a shaft element. The mesh size is 0.01m, thus comprising 100 elements and 101 nodes. This mesh is sufficient for convergence of the conducted modal analysis.

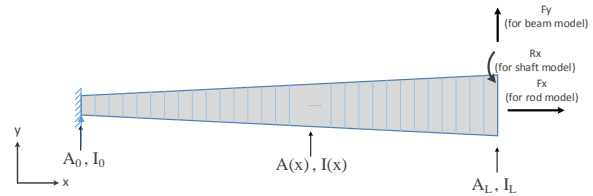


Figure 2. Tapered model used in the numerical experiment.

A matrix of cross-section areas, moments of inertia, and polar moments of inertia have to be constructed and used as input parameters. Each matrix has the values of radii r_0 and r_L , A_0 and A_L , I_0 and I_L , and J_0 and J_L , defined for each finite element of the used mesh. A computer program is built in MATLAB® environment for that purpose and for building the FEM model and solving the system of matrices. The Frequency Response Function (FRF) is then calculated at the excitation DOF. Different frequency ranges are used, depending on the type of waveguide, i.e., beam, rod, or shaft. The aim is to compare the first few natural frequencies of each waveguide.

The radii for the circular cross-section model used are: $r_0 = 10\text{mm}$ and $r_L = 30\text{mm}$. For the rectangular cross-section, a member's height of $h = 20\text{mm}$ is used, and smaller width of $b_0 = 20\text{mm}$, and bigger width of $b_L = 60\text{mm}$ are used in the analysis.

A. Idealization Using Uniform Elements

As an acceptable alternative, the obtained expressions are benchmarked by replacing the tapered member with a stepped element consisting of a sufficient number of rigidly connected uniform elements, as shown in Figure 3. The same element size used in the tapered element model is adopted.

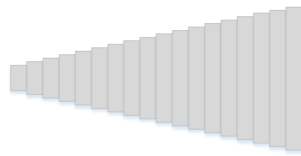


Figure 3. Idealization of tapered elements with uniform elements.

B. Comparisons of Obtained Natural Frequencies

The calculated natural frequencies are derived from the obtained FRFs and are shown in the following, benchmarked with the uniform model of each waveguide. These are demonstrated for the circular and rectangular cross-section types, as demonstrated in Table 1 and Table 2.

Table 1. (A) First Few Natural Frequencies in Hz: Circular Cross-sections (Beam & Rod Elements).

Mode No.	Beam Element		Rod Element	
	Uniform	Tapered (difference %)	Uniform	Tapered (difference %)
1	8.51	8.65 (1.65%)	772.3	777.1 (0.63%)
2	119.9	120.50 (0.50%)	3668.83	3669.6 (0.02%)
3	426.7	427.50 (0.19%)	6241.9	6242.36 (0.01%)
4	871.6	873.10 (0.17%)	8788.53	8788.85 (0.004%)
5	1463.5	1465.80 (0.16%)	11328.3	11328.60 (0.003%)
6	2202.8	2206.10 (0.15%)	13866.9	13867.10 (0.001%)

Table 1. (B) First Few Natural Frequencies in Hz: Circular Cross-sections (Shaft Element).

Mode No.	Shaft Element	
	Uniform	Tapered (difference %)
1	258.33	262.4 (1.59%)
2	2338.7	2336.5 (0.09%)
3	3912.8	3911.4 (0.04%)
4	5481	5480.1 (0.02%)
5	7049.6	7049.0 (0.01%)
6	8619.6	8619.3 (0.003%)

Table 2. (a) First Few Natural Frequencies in Hz: Rectangular Cross-sections (Beam & Rod Elements).

Mode No.	Beam Element		Rod Element	
	Uniform	Tapered (difference %)	Uniform	Tapered (difference %)
1	1.64	1.64 (0.01%)	1002.3	1005.1 (0.28%)
2	13.02	13.02 (0.06%)	3701.2	3702.2 (0.03%)
3	39.07	39.07 (0.02%)	6259.7	6260.3 (0.01%)
4	77.88	77.88 (0.01%)	8800.9	8801.3 (0.005%)
5	129.64	129.6 (0.01%)	11337.8	11338.1 (0.003%)
6	194.37	194.3 (0.00%)	13874.6	13874.8 (0.001%)

Table 2. (B) (a) First Few Natural Frequencies in Hz: Rectangular Cross-sections (Shaft Element).

Mode No.	Shaft Element	
	Uniform	Tapered (difference %)
1	414.7	461.3 (11.24%)
2	2291.5	2210.0 (3.56%)
3	3881.5	3817.3 (1.65%)
4	5458	5405.6 (0.96%)
5	7031.4	6987.3 (0.63%)
6	8604.7	8566.7 (0.44%)

From the tables, all the natural frequencies calculated via tapered elements using the proposed formulation compare very well with the approximated model with a large number of uniform members, with very low differences.

V. CONCLUDING REMARKS

Direct formulas have been presented to calculate the mass and stiffness matrices for tapered finite elements. Formulations are carried out for beam, bar, and shaft elements. These formulations are based on the estimation of a function for the variation of the cross-sectional area, the moment of inertia, and the polar moment of inertia, for the analyzed elements. The main advantage of these formulas is their direct and simple utilization for the analysis of 3D types of truss structures that include tapered type of members. Benchmarking proved the effectiveness of the presented formulas and confirmed their reliability. A more complex expressions for arbitrary tapered cross sections can still be formulated but would probably result into longer and more complex mathematical formulations for the mass and stiffness matrices, which was not the idea in the present paper.

REFERENCES

- [1] C. K. Wang, "Stability of Rigid Frames with Nonuniform Members", *Journal of the Structure Division*. vol. 93, pp. 275-294, 1967.
- [2] J. F. Doyle, *Wave Propagation in Structures*, New York, Springer-Verlag, 1989.
- [3] V. Kolousek, *Dynamics of engineering structures*, New York, Halsted press, 1973.
- [4] Robert D. Blevins, *Formulas for dynamics, acoustics and vibration*, John Wiley & Sons Ltd, 2015.
- [5] R. S. Langley, "Wave evolution, reflection, and transmission along inhomogeneous waveguides". *Journal of Sound and Vibration*, 227, pp. 131-158, 1999.
- [6] N. Bazeos and D. L. Karabalis, "Efficient Computation of Buckling Loads for Plane Steel Frames with Tapered Members". *Engineering Structures*. vol. 28 pp. 771-775, 2006.
- [7] M. Cem Ece, M. Aydogdu, V. Taskin, "Vibration of a variable cross-section beam", *Mechanics Research Communications*, vol. 34, Issue 1, pp. 78-84, 2007.
- [8] T. T. Huong and B. S. Gan, "Development of Consistent Shape Functions for linearly solid Tapered Timoshenko Beam", *Journal of Structural and Construction Engineering (Transactions of AIJ)*, vol. 80(713), pp. 1103-1111, 2015.
- [9] F. Mohri, S. Meftah, N. Damil, "A large torsion beam finite element model for tapered thin-walled open cross sections beams", *Engineering Structures*, vol. 99, pp. 132-148, 2015.
- [10] M. K. Kalkowski, J. M. Muggleton and E. Rustighi, "Wave propagation in rods with an exponentially varying cross-section -

modelling and experiments", Journal of Physics: Conference Series 744, 2016.

[11] J.R. Banerjee and A. Ananthapurvirajah, "Free flexural vibration of tapered beams", Computers & Structures, vol. 224, 2019.

[12] S. N. Chockalingam, M. Nithyadharan and V. Pandurangan, "Shear stress distribution in tapered I-beams: Analytical expression and finite element validation", Thin-Walled Structures, vol. 157, 2020.

[13] M. Soltani and A. Soltani, "An Efficient Approach into Finite Element Method for Lateral Buckling Analysis of Fiber-Metal Laminates Tapered I-Beams", Periodica Polytechnica Civil Engineering, vol. 66(3), pp. 978–989, 2022.

[14] J. F. Doyle, *Static and Dynamic Analysis of Structures with An Emphasis on Mechanics and Computer Matrix Methods*. Springer-Science, 1991.

[15] Klaus-Jürgen Bathe, *Finite Element Procedures*, 2nd ed., Prentice Hall, 2014.

BIOGRAPHY

Dr. Khaled M. Ahmida Al-Ashouri received his BSc in Nuclear Engineering from the University of Tripoli. He received his MSc in Mechanical Engineering from the State University of Campinas Unicamp in 1996 in the area of applied and computational mechanics. In 2001, he received his Ph.D. degree in Mechanical Engineering from the same university in the area of structural vibrations and acoustics. Later he spent some time as a postdoctoral fellow and worked for many years as a researcher at Unicamp. He is currently a professor at the Department of Mechanical and Industrial Engineering, at the University of Tripoli. His research work focuses on mechanical vibrations and acoustics, finite element analysis, and structural health monitoring.

APPENDIX

Appendix A: tapered elements with circular cross-section

The stiffness and mass matrices are symmetric, and their elements are as follows.

A1: Linearly tapered beam element:

$$K_B^{Lc}(1,1) = \frac{3E\pi(11r_0^4 + 5r_0^3r_L + 3r_0^2r_L^2 + 5r_0r_L^3 + 11r_L^4)}{35L^3}$$

$$K_B^{Lc}(1,2) = \frac{E\pi(47r_0^4 + 22r_0^3r_L + 9r_0^2r_L^2 + 8r_0r_L^3 + 19r_L^4)}{70L^2}$$

$$K_B^{Lc}(1,3) = -\frac{3E\pi(11r_0^4 + 5r_0^3r_L + 3r_0^2r_L^2 + 5r_0r_L^3 + 11r_L^4)}{35L^3}$$

$$K_B^{Lc}(1,4) = \frac{E\pi(19r_0^4 + 8r_0^3r_L + 9r_0^2r_L^2 + 22r_0r_L^3 + 47r_L^4)}{70L^2}$$

$$K_B^{Lc}(2,2) = \frac{E\pi(17r_0^4 + 9r_0^3r_L + 4r_0^2r_L^2 + 2r_0r_L^3 + 3r_L^4)}{35L}$$

$$K_B^{Lc}(2,3) = -\frac{E\pi(47r_0^4 + 22r_0^3r_L + 9r_0^2r_L^2 + 8r_0r_L^3 + 19r_L^4)}{70L^2}$$

$$K_B^{Lc}(2,4) = \frac{E\pi(13r_0^4 + 4r_0^3r_L + r_0^2r_L^2 + 4r_0r_L^3 + 13r_L^4)}{70L}$$

$$K_B^{Lc}(3,3) = \frac{3E\pi(11r_0^4 + 5r_0^3r_L + 3r_0^2r_L^2 + 5r_0r_L^3 + 11r_L^4)}{35L^3}$$

$$K_B^{Lc}(3,4) = -\frac{E\pi(19r_0^4 + 8r_0^3r_L + 9r_0^2r_L^2 + 22r_0r_L^3 + 47r_L^4)}{70L^2}$$

$$K_B^{Lc}(4,4) = \frac{E\pi(3r_0^4 + 2r_0^3r_L + 4r_0^2r_L^2 + 9r_0r_L^3 + 17r_L^4)}{35L}$$

$$M_B^{Lc}(1,1) = \frac{\rho\pi L(145r_0^2 + 70r_0r_L + 19r_L^2)}{630}$$

$$M_B^{Lc}(1,2) = \frac{\rho\pi L^2(65r_0^2 + 50r_0r_L + 17r_L^2)}{2520}$$

$$M_B^{Lc}(1,3) = \frac{\rho\pi L(23r_0^2 + 35r_0r_L + 23r_L^2)}{630}$$

$$M_B^{Lc}(1,4) = -\frac{\rho\pi L^2(25r_0^2 + 34r_0r_L + 19r_L^2)}{2520}$$

$$M_B^{Lc}(2,2) = \frac{\rho\pi L^3(5r_0^2 + 5r_0r_L + 2r_L^2)}{1260}$$

$$M_B^{Lc}(2,3) = \frac{\rho\pi L^2(19r_0^2 + 34r_0r_L + 25r_L^2)}{2520}$$

$$M_B^{Lc}(2,4) = -\frac{\rho L^3\pi\left(r_0^2 + \frac{8}{5}r_0r_L + r_L^2\right)}{504}$$

$$M_B^{Lc}(3,3) = \frac{\rho\pi L(19r_0^2 + 70r_0r_L + 145r_L^2)}{630}$$

$$M_B^{Lc}(3,4) = -\frac{\rho\pi L^2(17r_0^2 + 50r_0r_L + 65r_L^2)}{2520}$$

$$M_B^{Lc}(4,4) = \frac{\rho\pi L^3(2r_0^2 + 5r_0r_L + 5r_L^2)}{1260}$$

A2: Linearly tapered rod element:

$$K_R^{Lc} = \begin{bmatrix} \frac{E\pi(r_0^2 + r_0r_L + r_L^2)}{3L} & -\frac{E\pi(r_0^2 + r_0r_L + r_L^2)}{3L} \\ \text{symmetric} & \frac{E\pi(r_0^2 + r_0r_L + r_L^2)}{3L} \end{bmatrix}$$

$$M_R^{Lc} = \begin{bmatrix} \frac{\rho\pi L(6r_0^2 + 3r_0r_L + r_L^2)}{30} & \frac{\rho\pi L(3r_0^2 + 4r_0r_L + 3r_L^2)}{60} \\ \text{symmetric} & \frac{\rho\pi L(r_0^2 + 3r_0r_L + 6r_L^2)}{30} \end{bmatrix}$$

A3: Linearly tapered shaft element:

$$K_S^{Lc} = \begin{bmatrix} \frac{G\pi(r_0^4 + r_0^3r_L + r_0^2r_L^2 + r_0r_L^3 + r_L^4)}{10L} & -\frac{G\pi(r_0^4 + r_0^3r_L + r_0^2r_L^2 + r_0r_L^3 + r_L^4)}{10L} \\ \text{symmetric} & \frac{G\pi(r_0^4 + r_0^3r_L + r_0^2r_L^2 + r_0r_L^3 + r_L^4)}{10L} \end{bmatrix}$$

$$M_S^{Lc} = \begin{bmatrix} \frac{\rho\pi L(15r_0^4 + 10r_0^3r_L + 6r_0^2r_L^2 + 3r_0r_L^3 + r_L^4)}{210} & \frac{\rho\pi L(5r_0^4 + 8r_0^3r_L + 9r_0^2r_L^2 + 8r_0r_L^3 + 5r_L^4)}{420} \\ \text{symmetric} & \frac{\rho\pi L(r_0^4 + 3r_0^3r_L + 6r_0^2r_L^2 + 10r_0r_L^3 + 15r_L^4)}{210} \end{bmatrix}$$

Appendix B: tapered elements with rectangular cross-section

The stiffness and mass matrices are symmetric, and their elements are as follows.

B1: Linearly tapered beam element:

$$K_B^{Lr} = \begin{bmatrix} \frac{6E(I_0 + I_L)}{L^3} & \frac{2E(2I_0 + I_L)}{L^2} & -\frac{6E(I_0 + I_L)}{L^3} & \frac{2E(I_0 + 2I_L)}{L^2} \\ & \frac{E(3I_0 + I_L)}{L} & -\frac{2E(2I_0 + I_L)}{L^2} & \frac{E(I_0 + I_L)}{L} \\ & & \frac{6E(I_0 + I_L)}{L^3} & -\frac{2E(I_0 + 2I_L)}{L^2} \\ \text{symmetric} & & & \frac{E(I_0 + 3I_L)}{L} \end{bmatrix}$$

$$M_B^{Lr} = \begin{bmatrix} \frac{\rho L(10A_0 + 3A_L)}{35} & \frac{\rho L^2(15A_0 + 7A_L)}{420} & \frac{9\rho L(A_0 + A_L)}{140} & -\frac{\rho L^2(7A_0 + 6A_L)}{420} \\ & \frac{\rho L^3(5A_0 + 3A_L)}{840} & \frac{\rho L^2(6A_0 + 7A_L)}{420} & -\frac{\rho L^3(A_0 + A_L)}{280} \\ & & \frac{\rho L(3A_0 + 10A_L)}{35} & -\frac{\rho L^2(7A_0 + 15A_L)}{420} \\ \text{symmetric} & & & \frac{\rho L^3(3A_0 + 5A_L)}{840} \end{bmatrix}$$

B2: Linearly tapered rod element:

$$K_R^{Lr} = \begin{bmatrix} \frac{E(A_0 + A_L)}{2L} & -\frac{E(A_0 + A_L)}{2L} \\ \text{symmetric} & \frac{E(A_0 + A_L)}{2L} \end{bmatrix}$$

$$M_R^{Lr} = \begin{bmatrix} \frac{\rho L(3A_0 + A_L)}{12} & \frac{\rho L(A_0 + A_L)}{12} \\ \text{symmetric} & \frac{\rho L(A_0 + 3A_L)}{12} \end{bmatrix}$$

B3: Linearly tapered shaft element:

$$K_S^{Lr} = \begin{bmatrix} \frac{G(J_0 + J_L)}{2L} & -\frac{G(J_0 + J_L)}{2L} \\ \text{symmetric} & \frac{G(J_0 + J_L)}{2L} \end{bmatrix}$$

$$M_S^{Lr} = \begin{bmatrix} \frac{\rho L(3J_0 + J_L)}{12} & \frac{\rho L(J_0 + J_L)}{12} \\ \text{symmetric} & \frac{\rho L(J_0 + 3J_L)}{12} \end{bmatrix}$$